Available online at www.sciencedirect.com
SCIENCE DIRECT®
Journal of Molecular Catalysis A: Chemical 221 (2004) 89–95
JOURNAL OF MOLECULAR CATALYSIS A: CHEMICAL
www.elsevier.com/locate/molcata

Auto-reduction of Cu(II) species supported on Al_2O_3 to Cu(I) by thermovacuum treatment

Fumiaki Amano, Tsunehiro Tanaka*, Takuzo Funabiki

Department of Molecular Engineering, Graduate School of Engineering, Kyoto University, Kyoto 615-8510, Japan

Received 28 February 2004; received in revised form 21 June 2004; accepted 21 June 2004
Available online 30 July 2004

Abstract

We investigated the reduction behavior of Cu^{2+} species supported on γ-Al_2O_3 in vacuo at high temperature by combined use of electron paramagnetic resonance (EPR) detecting highly dispersed Cu^{2+} species and photoluminescence spectroscopy monitoring isolated Cu^{+} ions. In the case of low loaded alumina-supported copper catalysts (Cu^{2+}/Al_2O_3), there are isolated Cu^{2+} species centered in tetragonal distorted octahedra. It was found that the isolated Cu^{2+} species are easily reduced to Cu^{+} ions by thermovacuum treatment for Al_2O_3-supported catalyst, which are different from the past report for copper exchanged zeolites. On the other hand, the less dispersed Cu^{2+} species cannot be fully reduced to Cu^{+} ions in vacuo at 973 K on the alumina surface.

Keywords: Autoreduction; Thermal self-reduction; CuO/Al_2O_3; Cu-ZSM-5; Phosphorescence emission

1. Introduction

Cu^{2+} species supported on zeolites or metal oxides promote the selective catalytic reduction (SCR) of nitrogen oxides [1,2]. In particular, a Cu^{2+} ion exchanged ZSM-5 zeolite catalyst (Cu-ZSM-5) is widely investigated, because that exhibits a high catalytic activity in the direct NO decomposition and the SCR with hydrocarbons [3]. The redox properties of Cu^{2+} ions play an important role in the catalytic activity. The Cu^{2+} ions supported on ZSM-5 are known to be reduced to Cu^{+} ions thermally, without a reductant such as H_2 and CO, in vacuo or under an inert gas flow at high temperature [4–6]. This phenomenon is called "auto-reduction" or "self-reduction". Liu and Robota [4] observed the correlation between the thermally reduced Cu^{+} ion concentration in Cu-ZSM-5 and the NO decomposition rate.

The thermal reduction of Cu^{2+} ions has been assumed to proceed as follows; $Cu^{2+}(OH^{-})$ species are condensed by dehydration followed by the formation of Cu^{2+}–O^{2-}–Cu^{2+} dimer or oligomer species and the bridging extra-lattice oxygen atoms are desorbed as oxygen molecules accompanied by reduction of Cu^{2+} ions to Cu^{+} ions [5,6]. Larsen et al. [7] proposed another mechanism; the auto-reduction of Cu^{2+} ions are accompanied by the water desorption because the electron paramagnetic resonance (EPR) signal intensities decreased by thermal treatment at 473 K and restored by dosed water at room temperature. On the other hand, Hall and co-workers [8] confirmed that the decrease in the EPR signal intensities at 473 K is not due to the auto-reduction but due to a change of Cu^{2+} ions circumstances to low symmetry resulting from dehydration by means of magnetic measurement. Lamberti and co-workers [9] have also reported that the thermal reduction to Cu^{+} ions never occurs at 470 K but does occur at 670 K. They considered that EPR silent species such as Cu^{2+} dimer species or low coordinated Cu^{2+} species formed in the early stages of water desorption.

There have been many studies on the redox behavior of Cu species supported on zeolites or silica. It is known that Cu^{2+} species dispersed on silica materials such as ZSM-5, Y-zeolite [10], mordenite [11–13], and SiO_2 [14] are auto-reduced to Cu^{+} ions by thermal treatment. Kuroda et al. [15] have re-

* Corresponding author. Tel.: 81 75 383 2562; fax: 81 75 383 2561.
E-mail address: tanaka@dcc.mbox.media.kyoto-u.ac.jp (T. Tanaka).

1381-1169/$ – see front matter © 2004 Elsevier B.V. All rights reserved.
doi:10.1016/j.molcata.2004.06.014

ported that Cu^{2+} species dispersed on silica-alumina having lower Si/Al ratio are prevented from the auto-reduction. They proposed that the resistance to the auto-reduction was responsible for the stabilization of Cu^{2+} cations by paired ion-exchangeable sites. However, the effects of support materials and Cu dispersion on the thermal reduction behavior of Cu species under vacuum have not been fully clarified.

We have found that an alumina supported Cu^{2+} (Cu^{2+}/Al_2O_3) catalyst promotes the selective catalytic reduction of NO with CO in the presence of O_2 [16]. Diffuse reflectance UV–vis/NIR and XANES spectra of the highly active catalyst show that the Cu^{2+} species are in a distorted octahedral coordination and highly dispersed form on the γ-Al_2O_3 surface [17]. In the present study, we have found the thermal reduction of isolated Cu^{2+} ions to Cu^{+} on the γ-Al_2O_3 surface. It is merely known the auto-reduction of Cu^{2+} species supported on ionic metal oxides such as γ-Al_2O_3 in contrast to SiO_2-based support such as zeolites. We investigated the reducibility of the highly dispersed Cu^{2+} species on γ-Al_2O_3 in vacuo at high temperature by means of EPR and photoluminescence spectroscopies.

2. Experimental

The alumina-supported Cu^{2+} catalysts were prepared by impregnation of γ-Al_2O_3 (JRC–ALO–8, 148 $m^2\,g^{-1}$) provided by the Catalysis Society of Japan with an aqueous solution of $Cu(NO_3)_2$ at 353 K. The samples were pressed to disks followed by calcination at 773 K in dry air. The calcined disks were crushed to 26–50 mesh in a mortar. We prepared catalysts of different Cu loadings, 0.1, 0.25, 0.5, 0.75, 1, 3 and 5 wt.%, as copper metal, in order to reveal the relationship between the degree of Cu dispersion and reducibility. In the case of copper loading of more than 10 wt.%, the supported Cu^{2+} species are aggregated to bulk CuO crystallites on γ-Al_2O_3 surface by the calcination at moderate temperature and are transformed to bulk $CuAl_2O_4$ crystallites by calcination at 973 K [17]. The calcined samples were kept in a hydrated state under ambient condition. In this study, we assigned loading amount of 0.1–0.75 wt.% as low loaded catalysts and loading amount of 1.0–5.0 wt.% as highly loaded catalysts.

The X-band EPR spectra were recorded with a JES-SRE2X spectrometer (JEOL) at room temperature. The g factor was determined by using an Mn^{2+} marker included in MgO. The signal intensity of EPR spectra was calculated from twice integration.

The photoluminescence measurements were performed with a LS50B spectrometer (Perkin-Elmer) at room temperature. The emission and excitation spectra were recorded in the phosphorescence mode with a delayed time of 50 μs. The life times were evaluated from the exponential curve fittings of the decay of the phosphorescence emission intensity.

Prior to each measurement, the hydrated samples were thermally treated at various temperatures under 3×10^{-3} Torr for 2 h and cooled down to room temperature in vacuo. The samples were sealed out in a quartz tube without exposure to air after the thermovacuum treatments.

3. Results and discussion

3.1. The Cu^{2+} dispersion of Cu^{2+}/Al_2O_3 catalysts

XRD patterns of Cu-related compounds such as bulk CuO and $CuAl_2O_4$ crystallites are not detected on any Cu^{2+}/Al_2O_3 catalyst [16]. The UV–vis/NIR spectra of each Cu^{2+}/Al_2O_3 catalyst show the d–d transition of Cu^{2+} ions in a distorted octahedral coordination [17]. These results suggest that the Cu^{2+} species supported on γ-Al_2O_3 are in a highly dispersed form different from CuO-like clusters. Isolated Cu^{2+} species on γ-Al_2O_3 are often called superficial copper-aluminate spinel species because the Cu^{2+} species are assumed to occupy the octahedral cation vacant site of the γ-Al_2O_3 surface [18,19]. However, the structure of $CuAl_2O_4$ crystallites is random spinel consisting of the Cu^{2+} ions of 60% tetrahedral and 40% octahedral coordination [20]. The local environment of the Cu^{2+} species called superficial spinel is different from bulk $CuAl_2O_4$ spinel obviously [21].

The local structures of cupric ($3d^9$) paramagnetic ions are characterized by means of EPR spectroscopy. Fig. 1 shows the EPR spectra of Cu^{2+}/Al_2O_3 catalysts evacuated at room temperature. In the case of 0.1 wt.% Cu^{2+}/Al_2O_3 catalyst, the spectrum was typical of Cu^{2+} cations in an axial symmetry [7,22–24]. Four splitting features (m_I = −3/2, −1/2, 1/2, 3/2) due to the hyperfine interaction between the unpaired electron and the nuclear spin of Cu (I = 3/2) appear on the

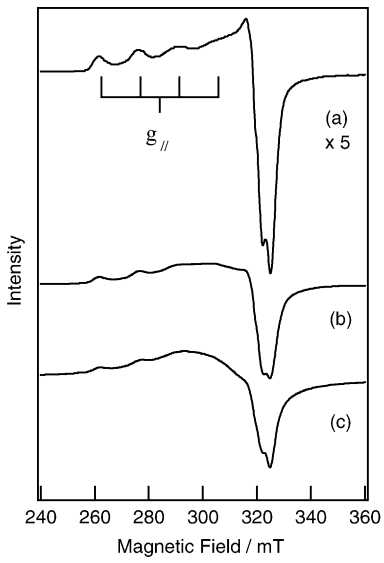

Fig. 1. EPR spectra of Cu^{2+}/Al_2O_3 catalysts evacuated at room temperature: (a) 0.1 wt.%; (b) 0.5 wt.%; and (c) 3.0 wt.%.

parallel component in the low field region. The anisotropic parameters ($g_{//}$ = 2.30, $A_{//}$ = 145 G) were in agreement with a tetragonally distorted octahedral symmetry reported for Cu^{2+}/Al_2O_3 samples [22,23,25]. The broadening of the parallel hyperfine features increases gradually with an increase in m_I, which can be attributed to correlated *g*- and *A*-strain results from a heterogeneity of micro-environments of the copper sites [24]. The signal of the perpendicular component was too broad to determine the anisotropic parameters clearly. This broadening was not a motional effect because the spectrum measured at 123 K was almost the same as that at room temperature. The perpendicular figures of 0.1 wt.% Cu^{2+}/Al_2O_3 catalyst were not perfectly simulated by one axial spin Hamiltonian. Lamberti et al. [26] have simulated the experimental EPR spectrum of an alumina supported $CuCl_2$ catalyst with a low Cu loading as the superimposition of two very close axial signals, suggesting the presence of two types in slightly different microenvironments. In the present sample, there would be several isolated Cu^{2+} species in very similar axial symmetry due to the heterogeneity of γ-Al_2O_3 surface.

A 0.5 wt.% Cu^{2+}/Al_2O_3 catalyst shows axially symmetric signals that have relatively broad line width and unresolved hyperfine features in comparison with the 0.1 wt.% Cu^{2+}/Al_2O_3 catalyst. The axial signals have two overlapping spectral components; the anisotropic signal of isolated Cu^{2+} species is superimposed by another broad anisotropic signal. The presence of neighboring Cu^{2+} species causes broadening of EPR signal due to dipole–dipole magnetic interaction between the paramagnetic sites [27]. We consider that the broad anisotropic signal is attributed to neighboring Cu^{2+} monomers that is very weakly interacted with each other.

The EPR signal intensities decrease extremely in the case of formation of aggregated Cu^{2+} species such as CuO clusters. The Cu–O–Cu networks are EPR inactive due to the strongly magnetic interaction. A 3.0 wt.% Cu^{2+}/Al_2O_3 catalyst shows very broad EPR signals mainly derived from neighboring Cu^{2+} monomers in anisotropic symmetry. To some extent, there might be overlapping of very weak isotropic signals resulting from Cu^{2+} aggregates. The signal intensity of the 3.0 wt.% sample is comparable to that of the 0.5 wt.% sample in spite of the high loading of copper. This result indicates the presence of EPR inactive species. Here, it is noteworthy that this EPR inactive Cu^{2+} clusters are different from bulky CuO-like species, because the local structures are found to be different from CuO crystallites even in the case of high loading (1.0–3.0 wt.%) region by means of XANES and UV–vis/NIR spectroscopies [17]. Therefore, we consider that the EPR inactive aggregates are very fine multinuclear clusters taking into account of results from the other spectroscopic techniques.

Fig. 2a shows the integrated EPR signal intensities of Cu^{2+}/Al_2O_3 catalysts with different Cu loadings after outgassing at room temperature. The signal intensities increased with an increase in the Cu loadings up to 0.75 wt.% and decreased when it exceeded 1.0 wt.%. Moving to highly loaded

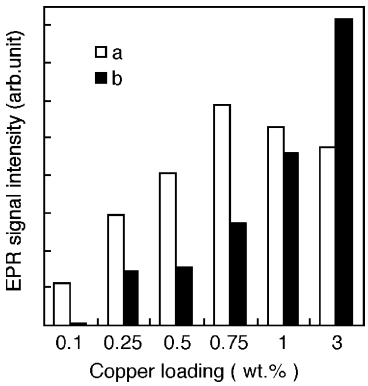

Fig. 2. The EPR signal intensities of Cu^{2+}/Al_2O_3 catalysts evacuated at: (a) room temperature; and (b) 973 K with different Cu loadings. The signal intensities are evaluated from twice integration of EPR spectra.

sample, the axial symmetry became broad and the hyperfine features unclear due to dipolar interaction between neighboring paramagnetic species. It is suggested that around 0.75 wt.%, the number of EPR active Cu^{2+} species were saturated on the γ-Al_2O_3 surface and that EPR inactive species started to be formed mainly. Therefore, we can decide the saturation point of highly dispersed Cu^{2+} species is around 0.75 wt.%, which corresponds to 0.5 wt.% Cu/100 m^2. If the cation vacant sites of the γ-Al_2O_3 are occupied, an excess Cu^{2+} species will begin to aggregate to form EPR inactive multinuclear species.

Fig. 3 shows a fraction of EPR active Cu^{2+} species of different Cu loaded catalysts. The spin densities are determined using $CuSO_4{\cdot}5H_2O$ as a standard. Although there are both the isolated and the neighboring Cu^{2+} species, the fraction of the EPR active species to the total amount of Cu can be regarded as a degree of the presence of highly dispersed Cu^{2+} species supported on γ-Al_2O_3. The fraction is evaluated from a twice integrated EPR signal intensity that is normalized to the number of Cu molecules contained in each catalyst, taking no thought of the difference in a signal intensity coefficient between the isolated ones and the neighboring ones. In the case of the 0.1 wt.% Cu^{2+}/Al_2O_3, the fraction of EPR active Cu^{2+} species were about 100% based on the total amount of

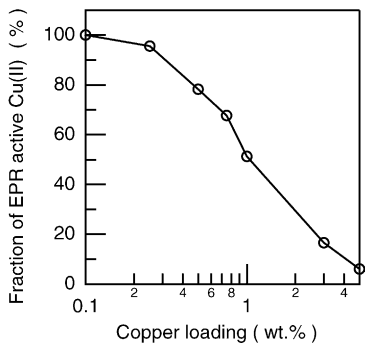

Fig. 3. The effects of copper loading on a fraction of EPR active Cu^{2+} species evaluated from the EPR signal intensity.

Cu in the sample. This indicates that all the Cu^{2+} species are captured by the cation vacant sites of the γ-Al_2O_3 surface in an isolated state. The fraction of the EPR active Cu^{2+} species decreased gradually with increasing Cu loadings. For highly loaded sample, 3.0–5.0 wt.%, the major species are the very fine Cu^{2+} aggregates instead of the monomers.

The EPR measurement of the Al_2O_3-supported Cu^{2+} catalysts revealed the dependence of loading amount for the Cu^{2+} dispersion. The two types of highly dispersed Cu^{2+} species in axial symmetry, which are the isolated monomers and the neighboring monomers, are dominant in the low loaded samples. The EPR active Cu^{2+} species interacting with each other are not Cu^{2+}–O^{2-}–Cu^{2+} dimers, because the copper dimer species are EPR silent in general. In addition, the dimers are difficult to be spread on γ-Al_2O_3 surface homogeneously taking into account thermodynamics. The Gibbs free energy ($G = H - TS$) of the surface monomers will be lower than that of the surface dimers as far as each enthalpy term (H) is almost the same, due to the higher entropy term (S) of monomers than dimers. In the highly loaded Cu catalysts, excess Cu^{2+} ions to the cation vacant sites of the γ-Al_2O_3 are aggregated to the very fine multinuclear species. Perhaps, a part of the aggregates show very weak EPR signals in isotropic symmetry.

3.2. Auto-reduction of the isolated Cu^{2+} species

Fig. 4 shows the EPR spectra of 0.1 wt.% Cu^{2+}/Al_2O_3 catalysts after evacuation at various temperatures. The EPR signal evacuated at lower temperature than 473 K was similar to that at room temperature. On the other hand, thermovacuum treatment at 773 K caused a variation of the signal shape and a little decrease in the EPR signal intensity. It is due to transformation of the local environment of hydrated Cu^{2+} species by desorption of coordinated hydroxyl groups [25].

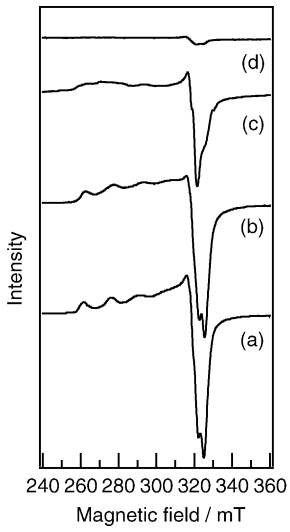

Fig. 4. EPR spectra of 0.1 wt.% Cu^{2+}/Al_2O_3 catalyst evacuated at: (a) room temperature; (b) 473 K; (c) 773 K; and (d) 973 K.

The EPR signal of the sample evacuated at 873 K was almost equivalent to that at 773 K.

After evacuation at 973 K, the EPR signal intensities decreased drastically and nearly disappeared. This disappearance in the signal suggests that the EPR active Cu^{2+} species are thermally reduced to $3d^{10}$ diamagnetic Cu^{+} ions. We can exclude the possibility of the formation of EPR inactive species such as the very fine Cu^{2+} aggregates after evacuation at 973 K, because the remaining signal shows a typical spectrum for Cu^{2+} species in axial symmetry. However, EPR spectroscopy cannot detect Cu^{+} species, so that another spectroscopic measurement is necessary for the precise characterization of the oxidation states of copper species.

The photoluminescence spectroscopy is a powerful tool in order to determine the presence of Cu^{+} ions. It is known that Cu^{+} ions show phosphorescence emissions that are affected by the local structures or the types of supported materials. The isolated Cu^{+} ions supported on zeolites are excited ($3d^{10} \rightarrow 3d^9 4p^1$) at 250–300 nm and exhibit the phosphorescence emission ($3d^9 4s^1 \rightarrow 3d^{10}$) at 450–550 nm [28–30]. Although the excitation bands of Cu^{+} ions have been assigned to the d–s transition ($3d^{10} \rightarrow 3d^9 4s^1$), the assignment is far from understanding, because the transition is dipole forbidden.

Fig. 5 shows emission spectra of 0.1 wt.% Cu^{2+}/Al_2O_3 catalysts excited by the light of 280 nm at room temperature. In the case of the sample evacuated at room temperature, no emission was detected. Evidently, isolated Cu^{+} ions are absent in the fresh Cu^{2+}/Al_2O_3 catalysts. Lifting evacuation temperature up to 773 K, a phosphorescent emission band emerged at 500 nm. Although not shown, the emission intensity of the sample evacuated at 873 K is almost consistent with that evacuated at 773 K. On the other hand, the evacuation at 973 K caused remarkable increase in the emission intensity. These emissions have been attributed to the photoluminescence from the isolated Cu^{+} ions supported on γ-Al_2O_3 with low-coordination number by means of X-ray absorption spectroscopy [31]. It is recognized that the disappearance in the EPR signal intensities after evacuation at 973 K is not due

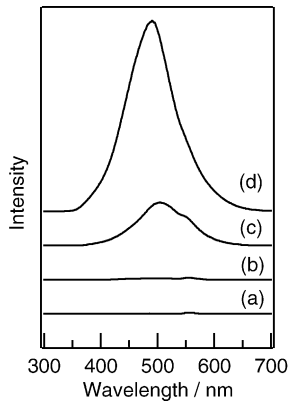

Fig. 5. Phosphorescence emission spectra of 0.1 wt.% Cu^{2+}/Al_2O_3 catalyst evacuated at: (a) room temperature; (b) 473 K; (c) 773 K; and (d) 973 K. The spectra were recorded at room temperature and monitored at 50 μs. Excitation wavelength was 280 nm.

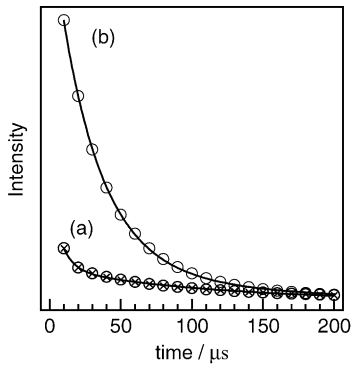

Fig. 6. Phosphorescence intensity decay of 0.1 wt.% Cu^{2+}/Al_2O_3 catalyst evacuated at: (a) 773 K; and (b) 973 K. Solid curves show the simulated decay curves. The spectra were recorded at room temperature. Emission spectra excited at 280 nm were monitored at 490 nm.

to a formation of EPR inactive Cu^{2+} species but due to a reduction to the isolated Cu^{+} ions. The presence of emission species after evacuation at 773 K shows that parts of the atomically dispersed Cu^{2+} species are thermally reduced to the isolated Cu^{+} ions. After evacuation at 973 K, the remaining Cu^{2+} species that resist to the auto-reduction at 773 K are also reduced to the Cu^{+} ions. There would be at least two types of isolated Cu^{2+} species supported on γ-Al_2O_3, easily auto-reducible ones at 773 K and less auto-reducible ones.

Fig. 6 shows the decay curves of the emission intensities of 0.1 wt.% Cu^{2+}/Al_2O_3 catalysts after thermal treatments in vacuo. The excitation wavelength was 280 nm and the intensity of the phosphorescence emission was monitored at 490 nm. The decay curve of the Cu^{+} emission in the sample evacuated at 773 K could be fitted using two sets of exponentials as below.

$$I = I_1 \exp\left(\frac{-t}{T_1}\right) + I_2 \exp\left(\frac{-t}{T_2}\right)$$

I_i is the band intensity of emission component i, T_i the lifetime of emission component i, and t the delayed time.

In the case of the sample evacuated at 773 K, the two components exhibit 8 and 108 μs life time. The decay curve of the sample evacuated at 973 K could be also fitted with short- and long-lived components. If we assume that the non-radiation process is negligible, the product of I_i and T_i can determine the fraction of the two emission sites. We obtained that the fractions of short- and long-lived components were 15 and 85%, respectively, in the sample evacuated at 773 K. On the other hand, in the case of the sample evacuated at 973 K, there were a large number of short-lived component (29 μs; 69%) in addition to long-lived component (108 μs; 31%). Although we cannot neglect non-radiation process actually, it is very likely that the amount of the isolated Cu^{+} species with short lifetime increased after evacuation at 973 K. In any cases, we can conclude that there exist several types of isolated Cu^{+} species in slightly different environments due to the heterogeneity of the γ-Al_2O_3 surface. The presence of two types of atomically dispersed Cu^{2+} species, easily auto-reducible one and less auto-reducible one at 773 K, might be correlated with the long-lived Cu^{+} species and the short-lived ones, respectively.

The isolated Cu^{+} species supported on ZSM-5 zeolite show two emission bands at 480 and 540 nm. Dedecek and Wichterlova [29] attributed the emission band at 480 nm (55 μs) to the Cu^{+} species adjacent to two Al framework atoms and the emission band at 540 nm (120 μs) to the Cu^{+} species adjacent to one Al framework atom, because the lower is the ratio of Si/Al, the more preferential is the emission band at 480 nm. Zecchina and co-workers [32] attributed the emission band at 480 nm to the Cu^{+} species coordinated to three oxygen atoms and the emission band at 540 nm to the Cu^{+} species coordinated to only two oxygen atoms. The coordination environments of the luminescence-active Cu^{+} species have not been clarified yet.

In the present case, each of the local environments of the Cu^{+} species is almost the same, because the wavelengths of the emission bands are not definitely different. However, the band max slightly shifts to 490 nm and a large number of the short lifetime species appeared after thermovacuum treatment at 973 K. This should be due to a slightly structural change around the Cu^{+} emission species into that exhibit stronger interaction with Al atoms, because the short-lived species increased with an increase in the content of Al ions in Cu-ZSM-5 [29]. Here, we confirmed that the highly dispersed Cu^{2+} species supported on γ-Al_2O_3 are auto-reducible to the isolated Cu^{+} ions with low coordination number by means of EPR and photoluminescence spectroscopy.

3.3. The effect of the Cu^{2+} dispersion on the auto-reducibility

Fig. 7 shows the photoluminescence emission spectra of Cu^{2+}/Al_2O_3 catalysts evacuated at 973 K with different Cu loadings. In the case of the low Cu-loaded catalysts (0.1–0.75 wt.%), the emission bands due to the isolated Cu^{+} ions ($3d^9 4s^1 \rightarrow 3d^{10}$) are clearly observed. On the other hand, the phosphorescence emission bands hardly emerge in the case of the highly Cu loaded catalysts (1.0–3.0 wt.%). It is considered that the Cu^{2+} species supported on γ-Al_2O_3 in a highly dispersed form are auto-reduced to the isolated Cu^{+} ions in vacuo at 973 K.

Fig. 8 shows the EPR spectra of Cu^{2+}/Al_2O_3 catalysts with different Cu loadings evacuated at 973 K. As shown in Fig. 4, the signal intensities nearly disappeared after evacuation at 973 K in the case of the 0.1 wt.% Cu^{2+}/Al_2O_3. The amount of the remaining Cu^{2+} species that are not reduced after evacuation at 973 K increased with Cu loadings. It seems that the less dispersed Cu^{2+} species supported on γ-Al_2O_3 resist to the auto-reduction into the isolated Cu^{+} ions, because the isolated Cu^{2+} species are thermally reduced to $3d^{10}$ diamagnetic ions (Fig. 8a). However, even in the case of the 0.5 wt.% Cu^{2+}/Al_2O_3, there are less auto-reducible ones at 973 K.

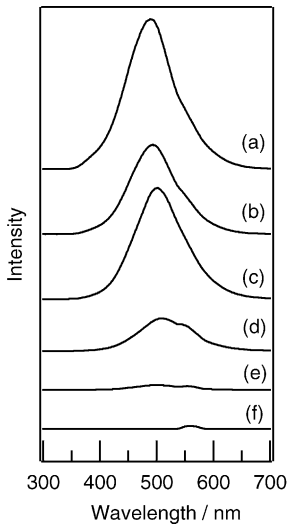

Fig. 7. Phosphorescence spectra of Cu^{2+}/Al_2O_3 catalysts evacuated at 973 K: (a) 0.1 wt.%; (b) 0.25 wt.%; (c) 0.5 wt.%; (d) 0.75 wt.%; (e) 1.0 wt.%; and (f) 3.0 wt.%. The spectra were recorded at room temperature and monitored at 50 μs. Excitation wavelength was 280 nm.

The comparison of twice-integrated EPR signal intensities between the fresh samples and the thermal treated ones at 973 K is presented in Fig. 2. For the low loaded catalysts, the EPR signal intensities decreased after evacuation at 973 K. For the highly loaded catalysts, the decrease at 973 K hardly occurs. Moreover, the signal intensity of 3.0 wt.% Cu^{2+}/Al_2O_3 increases after evacuation at 973 K as shown in Fig. 8f. It is suggested that the EPR inactive multinuclear species supported on γ-Al_2O_3 are hardly reduced but redispersed to EPR active Cu^{2+} species by thermal treatment. This behavior of the fine Cu^{2+} aggregates is also supported by the photoluminescence spectra; the intensities of photoemissions are very low in the case of the highly loaded samples. However, it is difficult to determine the amount of reduced Cu^+ species by means of photoemission spectra, because not all the Cu^+ ions show the phosphorescence emission bands due to various decay processes. Therefore, we cannot exclude the possibility of auto-reduction of the multinuclear Cu^{2+} species to Cu^+ ions. Actually, Praliaud et al. reported that the outgassing at 773 K reduces partially bulk CuO clusters creating Cu^+ ions in the CuO matrix (non-isolated Cu^+ ions) based on IR study of CO adsorption. In the same way, a part of fine multinuclear species in the present samples may undergo thermal reduction to Cu^+ ions surrounding by Cu^{2+} ions. However, we concluded that the fraction of the auto-reducible Cu^{2+} species to the total amount of copper would decrease with increasing Cu loadings on γ-Al_2O_3.

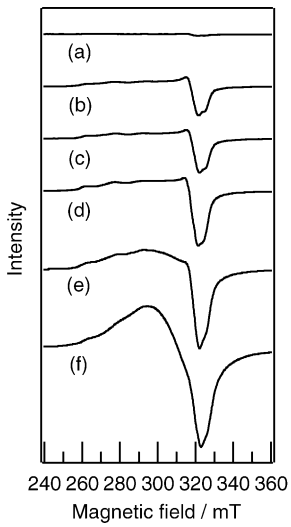

Fig. 8. EPR spectra of Cu^{2+}/Al_2O_3 catalysts evacuated at 973 K: (a) 0.1 wt.%; (b) 0.25 wt.%; (c) 0.5 wt.%; (d) 0.75 wt.%; (e) 1.0 wt.%; and (f) 3.0 wt.%.

It has been reported that the EPR signal intensities of alumina-supported catalyst with low Cu loadings decreased by thermal treatment under vacuum [33], and that low coordinated Cu^+ ions were formed by thermovacuum treatment starting from uncalcined 0.55 wt.% $Cu^{2+}(NO_3)_2/Al_2O_3$ catalyst [31]. However, this is the first report that has revealed that the isolated Cu^{2+} species supported on γ-Al_2O_3 are auto-reducible. It was suggested that the degree of the Cu^{2+} dispersion determines the auto-reducibility as a whole on γ-Al_2O_3 supported catalyst. The isolated Cu^{2+} ions are more easily reduced in vacuo on the γ-Al_2O_3 surface, which are different from the past report on zeolites and SiO_2 supported Cu^{2+} catalysts. For the copper exchanged ZSM-5 zeolites, it has been assumed that the auto-reduction of Cu^{2+} ions are promoted by desorption of bridging extra-lattice oxygen from Cu^{2+}–O^{2-}–Cu^{2+} dimer species [5,6,8]. However, the very fine multinuclear species, which possess the Cu^{2+}–O^{2-}–Cu^{2+} networks, supported on the γ-Al_2O_3 are less auto-reducible to the isolated Cu^+ ions.

Since the formation of the emission bands are accompanied by the decrease of EPR signal intensities, the Cu^{2+} monomers are reduced to the isolated Cu^+ ions without aggregation to the EPR inactive dimers. The full auto-reduction of the isolated Cu^{2+} ions has occurred at 973 K, so that the copper reduction would not be concomitant with water desorption. We also confirmed the reversible redox cycle of the isolated copper species under dry condition by means of EPR; Cu^{2+} ions re-oxidized by O_2 were reduced to Cu^+ ions by thermovacuum treatment at 973 K again. The mechanism of the thermal reduction should be as follows. The coordinated hydroxyl groups of the isolated Cu^{2+} ions are desorbed as water in the range 473–773 K. In the second step, evolution of two oxygen ligands as a molecular oxygen from the dehydrated Cu^{2+} monomer causes the thermal reduction into the low-coordinated Cu^+ ion.

4. Conclusions

The dispersion of the Cu^{2+} species is dependent on the Cu loadings over Al_2O_3-supported catalysts. In the case of

the low loaded region, two types of highly dispersed Cu^{2+} species exist in tetragonally distorted octahedral symmetry, isolated Cu^{2+} monomers and neighboring Cu^{2+} monomers. The excess Cu^{2+} species over the saturation point of γ-Al_2O_3 (0.5 wt.% Cu/100 m^2) aggregate to form EPR inactive multinuclear species.

We investigated the auto-reduction behavior of Cu^{2+} species supported on γ-Al_2O_3 by combined use of EPR and photoluminescence spectroscopy. It was found that the isolated Cu^{2+} monomers are easily reduced to the low-coordinated Cu^{+} ions by thermovacuum treatment for Al_2O_3-supported catalyst. On the other hand, the less dispersed Cu^{2+} species cannot be perfectly reduced to Cu^{+} ions in vacuo at 973 K. The degree of the Cu dispersion determines the auto-reducibility of Cu^{2+}/Al_2O_3 catalysts as a whole. This is the first report that has revealed the relationship between the Cu^{2+} dispersion and the auto-reducibility of Cu^{2+} ions supported on ionic metal oxides.

There are several types of thermally reducible Cu^{2+} monomers in Cu^{2+}/Al_2O_3 catalysts. It is also confirmed the formation of two types of thermally reduced Cu^{+} species; long- and short-lived emission species. The varieties of microenvironments of those copper species are probably due to the heterogeneity of the γ-Al_2O_3 surface as host material.

References

[1] G. Centi, S. Perathoner, Appl. Catal. A 132 (1995) 179.
[2] V.I. Parvulescu, P. Grange, B. Delmon, Catal. Today 46 (1998) 233.
[3] H. Yahiro, M. Iwamoto, Appl. Catal. A 222 (2001) 163.
[4] D.J. Liu, H.J. Robota, Catal. Lett. 21 (1993) 291.
[5] M. Iwamoto, H. Yahiro, K. Tanda, N. Mizuno, Y. Mine, S. Kagawa, J. Phys. Chem. 95 (1991) 3727.
[6] H.J. Jang, W.K. Hall, J. dItri, J. Phys. Chem. 100 (1996) 9416.
[7] S.C. Larsen, A. Aylor, A.T. Bell, J.A. Reimer, J. Phys. Chem. 98 (1994) 11533.
[8] M. LoJacono, G. Fierro, R. Dragone, X.B. Feng, J. dItri, W.K. Hall, J. Phys. Chem. B 101 (1997) 1979.
[9] G.T. Palomino, P. Fisicaro, S. Bordiga, A. Zecchina, E. Giamello, C. Lamberti, J. Phys. Chem. B 104 (2000) 4064.
[10] P.A. Jacob, W.D. Wilde, R.A. Schoonheydt, J.B. Uytterhoven, H. Beyer, J. Chem. Soc., Faraday Trans. 1 (1976) 1221.
[11] Y. Kuroda, Y. Yoshikawa, S. Konno, H. Hamano, H. Maeda, R. Kumashiro, M. Nagao, J. Phys. Chem. 99 (1995) 10621.
[12] H. Yamashita, M. Matsuoka, K. Tsuji, Y. Shioya, M. Anpo, M. Che, J. Phys. Chem. 100 (1996) 397.
[13] F. Xamena, P. Fisicaro, G. Berlier, A. Zecchina, G.T. Palomino, C. Prestipino, S. Bordiga, E. Giamello, C. Lamberti, J. Phys. Chem. B 107 (2003) 7036.
[14] M. Anpo, T. Nomura, T. Kitao, E. Giamello, M. Che, M.A. Fox, Chem. Lett. (1991) 889.
[15] Y. Kuroda, T. Mori, Y. Yoshikawa, S. Kittaka, R. Kumashiro, M. Nagao, Phys. Chem. Chem. Phys. 1 (1999) 3807.
[16] T. Yamamoto, T. Tanaka, R. Kuma, S. Suzuki, F. Amano, Y. Shimooka, Y. Kohno, T. Funabiki, S. Yoshida, Phys. Chem. Chem. Phys. 4 (2002) 2449.
[17] T. Yamamoto, T. Tanaka, S. Suzuki, R. Kuma, K. Teramura, Y. Kou, T. Funabiki, S. Yoshida, Top. Catal. 18 (2002) 113.
[18] M. Fernandez-Garcia, I. Rodriguez-Ramos, P. Ferreira-Aparicio, A. Guerrero-Ruiz, J. Catal. 178 (1998) 253.
[19] G. Leofanti, M. Padovan, M. Garilli, D. Carmello, A. Zecchina, G. Spoto, S. Bordiga, G.T. Palomino, C. Lamberti, J. Catal. 189 (2000) 91.
[20] R.M. Friedman, J.J. Freeman, F.W. Lytle, J. Catal. 55 (1978) 10.
[21] B.R. Strohmeier, D.E. Leyden, R.S. Field, D.M. Hercules, J. Catal. 94 (1985) 514.
[22] P.A. Berger, J.F. Roth, J. Phys. Chem. 71 (1967) 4307.
[23] A. Martinez-Arias, R. Cataluna, J.C. Conesa, J. Soria, J. Phys. Chem. B 102 (1998) 809.
[24] P.J. Carl, S.C. Larsen, J. Phys. Chem. B 104 (2000) 6568.
[25] D.B. Losee, A.J. Kassman, P.A. Wilson, J. Catal. 67 (1981) 226.
[26] C. Prestipino, S. Bordiga, C. Lamberti, S. Vidotto, M. Garilli, B. Cremaschi, A. Marsella, G. Leofanti, P. Fisicaro, G. Spoto, A. Zecchina, J. Phys. Chem. B 107 (2003) 5022.
[27] Y. Matsunaga, Bull. Chem. Soc. Jpn. 34 (1961) 1291.
[28] J. Texter, D.H. Strome, R.G. Herman, K. Klier, J. Phys. Chem. 81 (1977) 333.
[29] J. Dedecek, B. Wichterlova, J. Phys. Chem. 98 (1994) 5721.
[30] B. Wichterlova, J. Dedecek, A. Vondrova, J. Phys. Chem. 99 (1995) 1065.
[31] M. Matsuoka, W.S. Ju, K. Takahashi, H. Yamashita, M. Anpo, J. Phys. Chem. B 104 (2000) 4911.
[32] C. Lamberti, S. Bordiga, M. Salvalaggio, G. Spoto, A. Zecchina, F. Geobaldo, G. Vlaic, M. Bellatreccia, J. Phys. Chem. B 101 (1997) 344.
[33] G. Centi, S. Perathoner, D. Biglino, E. Giamello, J. Catal. 152 (1995) 75.